Nutrient supply to the surface waters of the North Atlantic: A model study

Andreas Oschlies
Institut für Meereskunde an der Universität Kiel, Kiel, Germany

Received 11 February 2000; revised 17 April 2001; accepted 17 April 2001; published 31 May 2002.

[1] An eddy-permitting coupled ecosystem-circulation model with accurate descriptions of advection and turbulent mixing is used to estimate the nitrate supply to the euphotic zone in the North and equatorial Atlantic Ocean. The simulated annual mean input of nitrate into the euphotic zone is separated into different supply routes, namely, turbulent vertical mixing, vertical advection, and horizontal transport. Vertical mixing is found to be the dominant supply mechanism in the subpolar North Atlantic, while horizontal advection provides most of the simulated nitrate input into the subtropical gyre. Contributions by vertical advection are largest in the equatorial upwelling region and in the subpolar gyre. A comparison with observational estimates of nitrate flux into euphotic zone of the subtropical gyre reveals that the model can simultaneously fit the estimates by *Lewis et al.* [1986] and *Jenkins* [1988] that were previously thought to be contradictory. The simulated nitrate supply is, on the other hand, not consistent with estimates of export production based on oxygen consumption [*Jenkins*, 1982]. The model results are used to investigate to what extent the advective input of organic matter could possibly explain a local imbalance between new and export production. It turns out that the simulated advective input of organic matter alone, which in the model provides nitrogen at a rate similar to that arising from nitrate supply, is not sufficient to explain observed oxygen consumption rates. *INDEX TERMS:* 4805 Oceanography: Biological and Chemical: Biogeochemical cycles (1615); 4845 Oceanography: Biological and Chemical: Nutrients and nutrient cycling; 4842 Oceanography: Biological and Chemical: Modeling; 4806 Oceanography: Biological and Chemical: Carbon cycling; *KEYWORDS:* nutrient supply, new production, export production, biological pump

1. Introduction

[2] The export of organic carbon from the ocean's surface toward its interior is a crucial process in the global carbon cycle. A result of this biologically mediated transport through the water column, the so-called biological pump, is the observed gradient in nutrients between the surface ocean, which is generally depleted, and deeper, nutrient-rich water. Without the biology acting the surface concentrations not only of nutrients but also of dissolved inorganic carbon would be much higher, resulting in much increased (approximately doubled) [e.g., *Sarmiento et al.*, 1990]) concentrations of atmospheric CO_2. Identifying what controls the fixation of organic carbon and its removal from the surface layers that are in direct contact with the atmosphere therefore is a key requisite for improving our understanding of the ocean's role in the global carbon cycle.

[3] Assuming nitrogen as the nutrient that limits biological production in the well-lit upper ocean, all primary production associated with the newly available nitrogen is called new production [*Dugdale and Goering*, 1967]. To the extent that atmospheric nitrogen supply, nitrogen fixation, and riverine input can be neglected, the export of photosynthetically fixed organic matter to the deep ocean has, in a steady state, to be balanced by an upward flux of nitrogen into the euphotic zone [*Eppley and Peterson*, 1979]. In this idealized situation, export and new production would be identical, though this balance does not need to hold locally because of horizontal transport of both inorganic and organic nitrogen within the euphotic zone.

0148-0227/02/2000JC000275

[4] In the present study a three-dimensional picture of nutrient supply to the upper North Atlantic is obtained by introducing a simple four-compartment nitrogen-based nitrate-phytoplankton-zooplankton-detritus (NPZD) pelagic ecosystem model into a high-resolution model of the North Atlantic circulation. The numerical model used is described in detail by *Oschlies and Garçon* [1999] (hereinafter referred to as OG99). An analysis of the large-scale patterns of annual primary production and surface chlorophyll concentrations as well as of the seasonal dynamics at selected Joint Global Ocean Flux Study (JGOFS) time series and process study sites [*Oschlies et al.*, 2000] (hereinafter referred to as OKG2000) identified two major deficiencies of this model: a more than an order of magnitude too low primary production in the subtropical gyre and unrealistically fast growing zooplankton stocks in middle and high latitudes that were needed to end the simulated phytoplankton spring bloom.

[5] Of particular concern is the model's failure to sustain observed levels of primary production in the subtropical gyre. A similar failure had previously been reported for a coarse-resolution model by *Sarmiento et al.* [1993], and it was originally hoped that a finer grid resolution and associated higher levels of mesoscale eddy activity would fix this model flaw. This hope was inspired by the conception of eddy-induced nitrate fluxes into the oligotrophic subtropical gyre, which had been put forward to explain apparent discrepancies among observational estimates of new production [*Jenkins*, 1988]. Observational evidence for individual eddy pumping events exists [*Falkowski et al.*, 1991; *McGillicuddy et al.*, 1998], and idealized process studies, for example by *Dadou et al.* [1996] and *McGillicuddy and Robinson* [1997], suggested a significant contribution of eddy-induced upwelling in oligotrophic regions of the ocean. However, enhancing the present high-resolution model's eddy activity to even higher and more realistic

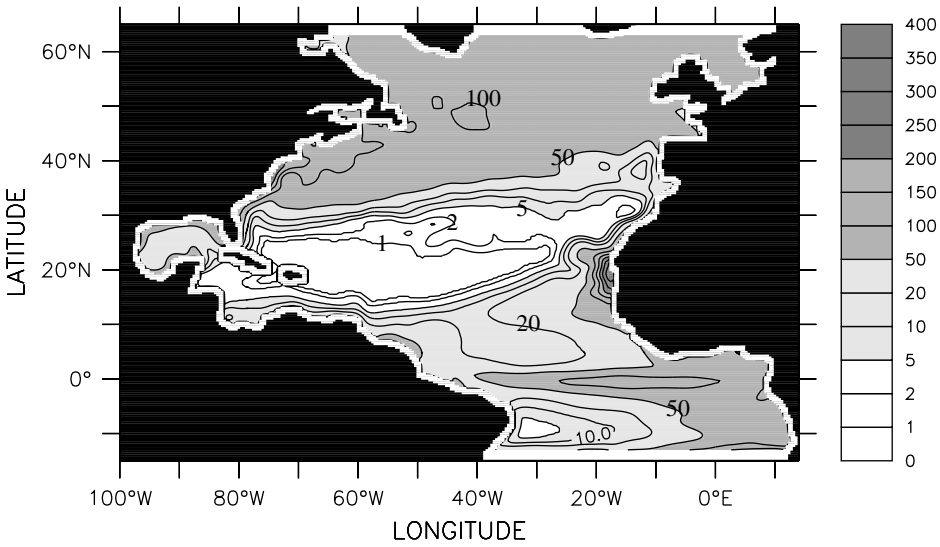

Figure 1. Simulated primary production averaged over years 3–7 of the coupled ecosystem-circulation model simulation. Units are g C m^{-2} yr^{-1}.

levels by assimilating TOPEX/Poseidon and ERS-1 altimetric data [*Oschlies and Garçon*, 1998] (hereinafter referred to as OG98) still showed the persistence of much too low levels of primary production in the subtropical gyre. It is not yet clear whether the underestimation in simulated primary production is caused mainly by too weak levels of new production or by too low levels of regenerated production. The present study attempts to clarify this issue by investigating how realistically the model simulates the nitrate input into the upper layer of the North Atlantic.

[6] After a brief description of the numerical model, section 3 focuses on the different physical mechanisms that supply nitrate to the surface waters of the North Atlantic. Section 4 addresses the "subtropical desert problem." Section 5 discusses the possible contribution of lateral transport of organic matter to explain discrepancies between methodologically different estimates of new production. Section 6 summarizes results and open issues.

2. Model Description

[7] The physical component of the coupled ecosystem-circulation model is based on the Geophysical Fluid Dynamics Laboratory's (GFDL) Modular Ocean Model (MOM) [*Pacanowski et al.*, 1991] primitive equation ocean circulation model. The present configuration is derived from the Community Modeling Effort (CME) model [*Bryan and Holland*, 1989] and covers the Atlantic Ocean between 15°S and 65°N with a grid spacing of 1/3° in meridional and 2/5° in zonal directions. While the original CME model had 30 levels in the vertical, a finer 37-level vertical grid is used for coupling with the simple nitrogen-based ecosystem model. Vertical mixing in and below the surface mixed layer is modeled by the turbulent kinetic energy (TKE) closure of *Gaspar et al.* [1990], with parameters chosen to match closely observations of diapycnal diffusion in the main thermocline [*Ledwell et al.*, 1993, 1998]. Below the surface mixed layer, vertical diffusivities K_ρ computed by the TKE scheme closely follow the relation $K_\rho = aN^{-1}$, where $a = 5.7 \times 10^{-4}$ cm^2 s^{-2} and N is the Brunt-Väisälä frequency. Such a dependence of K_ρ on N has been under debate for some time, and recent evidence suggests that diapycnal diffusivities may be independent of the buoyancy frequency in the stratified open ocean [*Polzin et al.*, 1995]. While modeled diffusivities agree well with in situ observations in the main thermocline ($K_\rho \approx 0.1$ cm^2 s^{-1}), simulated values in the strongly stratified seasonal thermocline below the summer mixed layer (but above the main thermocline) may become as small as 0.02 cm^2 s^{-1}. This would be too small if, in reality, K_ρ is independent of N, yielding $K_\rho = O(0.1$ cm^2 $s^{-1})$ everywhere in the open stratified ocean below the surface mixed layer and far away from the bottom. Although this issue is not completely resolved yet, it may nevertheless indicate an underestimation of simulated vertical diffusivities in the seasonal thermocline. The possible relevance to the modeled nutrient fluxes will be discussed below. Horizontal subgrid-scale diffusion and dissipation are parameterized by the highly scale selective biharmonic operator with mixing coefficients set to $A_h = 2.5 \times 10^{19}$ cm^4 s^{-1} for both momentum and tracers.

[8] Deviating from the model experiments described by OG99 and OKG2000, the atmospheric forcing consists of monthly mean wind stress and heat flux fields derived from the years 1989–1993 of the reanalysis project carried out at the European Centre for Medium-Range Weather Forecasts (ECMWF) [*Gibson et al.*, 1997]. Because precipitation fields were considered to be not yet reliable enough, freshwater fluxes were parameterized by restoring surface salinity to observed monthly means taken from the *Levitus et al.* [1994] atlas. Apart from the freshwater flux the ECMWF fields provide a consistent and as realistic as possible description of the atmospheric forcing. The formulation of the surface heat flux follows *Haney* [1971]. The downward heat flux into the ocean is expressed as

$$Q_{\mathrm{NET}}(T_{\mathrm{surf}}) = Q_{\mathrm{SOL}} + Q_{\mathrm{NSOL}} + Q_2(\mathrm{SST}_{\mathrm{obs}} - \mathrm{SST}_{\mathrm{mod}}). \quad (1)$$

Q_{SOL} and Q_{NSOL} account for solar and nonsolar heat fluxes as provided by the ECMWF reanalysis. $\mathrm{SST}_{\mathrm{obs}}$ is the observed weekly sea surface temperature (SST) field [*Reynolds and Smith*, 1994] that was also used in the ECMWF reanalysis. Q_2 represents the change of the surface heat flux per degree Celsius deviation of the simulated SST from the observed one. It has been computed from the 6 hourly reanalysis fields by a linear expansion of the surface heat flux bulk formulae [*Barnier et al.*, 1995]. The Q_2 term in (1) thus represents a physically plausible flux correction that accounts for a feedback from the simulated SST to the heat flux felt by the model ocean. In the experiments described in this study, Q_2 is taken to represent the climatological average computed over the 5 year period 1989–1993 and does not vary with time (though it does vary in space; see Figure 9). This was done particularly to allow a more straightforward intercomparison with experiments

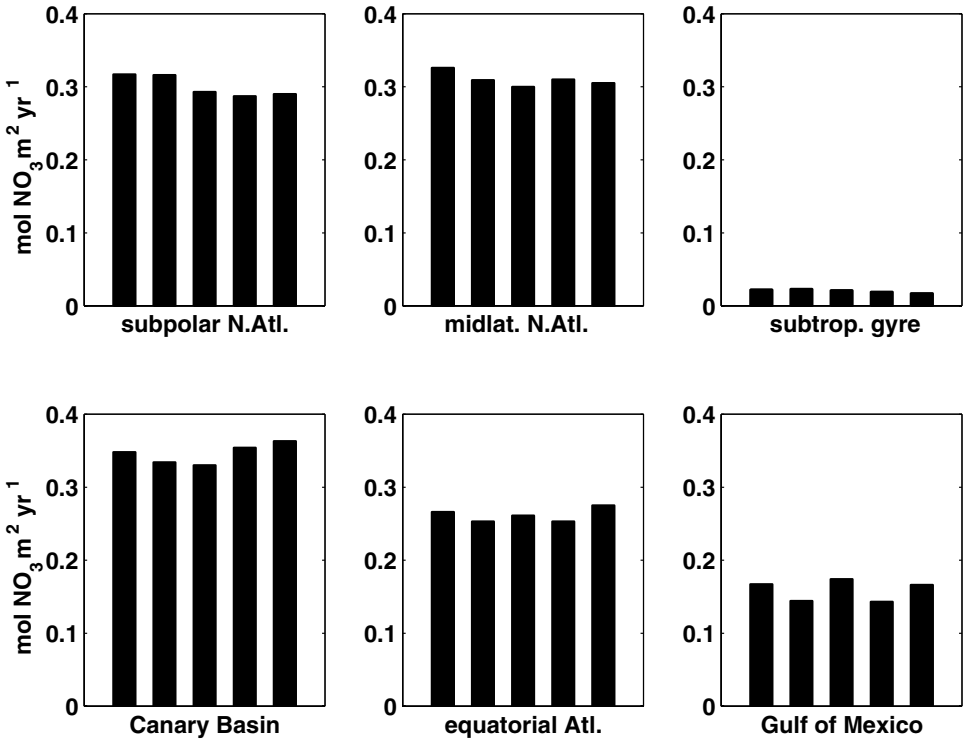

Figure 2. Simulated nitrate supply into the upper 126 m for different regions of the model: subpolar North Atlantic (50°–65°N), midlatitudinal North Atlantic (35°–50°N), subtropical gyre (15°–35°N, 70°–30°W), Canary Basin (8°–35°N, 30°W-coast), equatorial Atlantic (8°S–8°N), and the Gulf of Mexico (18°–32°N, 100°–82°W). The five vertical bars correspond to the simulated annual supply in the 5 consecutive years (years 3–7 of the coupled model run) used in the analysis. Units are mol m^{-2} yr^{-1}.

run with different forcing frequencies including daily forcing (not described in this study).

[9] Note that the 5 year period 1989–1993 from which the ECMWF data are taken falls into a phase marked by a relatively high index of the North Atlantic Oscillation (NAO) [*Hurrell*, 1995]. The older climatological data used in previous studies (OG98, OG99, and OKG2000) are, on the other hand, likely to be dominated by lower NAO indices that prevailed in the 1960s and 1970s. As argued by *Dickson et al.* [1996], winter convection near Bermuda and along the midlatitude storm track tends to be shallower in years with high NAO index. On the other hand, the strengthened Azores high-pressure system may intensify the upwelling off the African coast. Changes seen in the simulated primary production on switching to the ECMWF 1989–1993 forcing seem to be consistent with the above arguments: with respect to the results shown by OKG2000, primary production (Figure 1) is somewhat smaller in midlatitudes (by up to 30%) and slightly larger in the upwelling region off West Africa. Such changes are not important for the results presented in this paper, but for comparison with other investigations it should be kept in mind that the model's 1989–1993 forcing is biased toward a phase with high NAO index.

[10] Another difference from the model presented by OG99 is the treatment of nitrate at the artificially closed northern and southern walls where nitrate concentrations are now restored to the *Conkright et al.* [1994] climatology over a five grid point (5/3°) wide buffer zone. The restoring timescale decreases from 25 days at the innermost grid point to 5 days at the wall. This is the same timescale that is used for the restoring of temperature and salinity to monthly mean climatological values. No restoring is applied to phytoplankton, zooplankton, or detritus.

[11] The coupled model was started from a 25 year spin-up of the physical model only, which (different from OG99) already used the climatological (1989–1993) ECMWF forcing described above. After the biology was coupled in, an approximately stable seasonal cycle was reached after 2 years. The results shown below always represent 5 year averages over the coupled years 3–7. Typical interannual fluctuations of the simulated nitrate supply, which occur even under annually repeating climatological forcing as a result of internal model adjustment and variability, are shown for different regions in Figure 2. Over the 5 year period used in the analysis hereafter, none of the regional averages shows a significant trend. For the individual years, deviations of the simulated annual nitrate supply from the 5 year mean are always <10%. Throughout the paper a constant Redfield ratio of 6.625 mol C (mol N)$^{-1}$ will be used to convert nitrogen to carbon.

3. Physical Mechanisms Regulating the Large-Scale Pattern of Nitrate Supply

[12] The simulated input of nitrate into the upper 126 m of the model, which may be regarded as equivalent to the euphotic zone, is shown in Figure 3. Large regional differences can be identified, with supply rates lower than 0.01 mol N m^{-2} yr^{-1} (and even negative rates explained below) in the subtropics to rates exceeding 0.5 mol N m^{-2} yr^{-1} in the Gulf Stream region, along the equator, and off West Africa. The large regional differences in the nitrate supply are a result of different supply mechanisms being active in different regions, as shown in Figure 4. Vertical turbulent mixing, which in the model diagnostics includes convective overturning, provides a net upward transport of nitrate almost everywhere in the model domain (Figure 4a), reflecting the general increase of nitrate concentrations with depth. The subpolar region where nitrate supply by vertical mixing is large (>0.2 mol N m^{-2} yr^{-1}) has a well-defined southern boundary that closely follows the rather abrupt step in

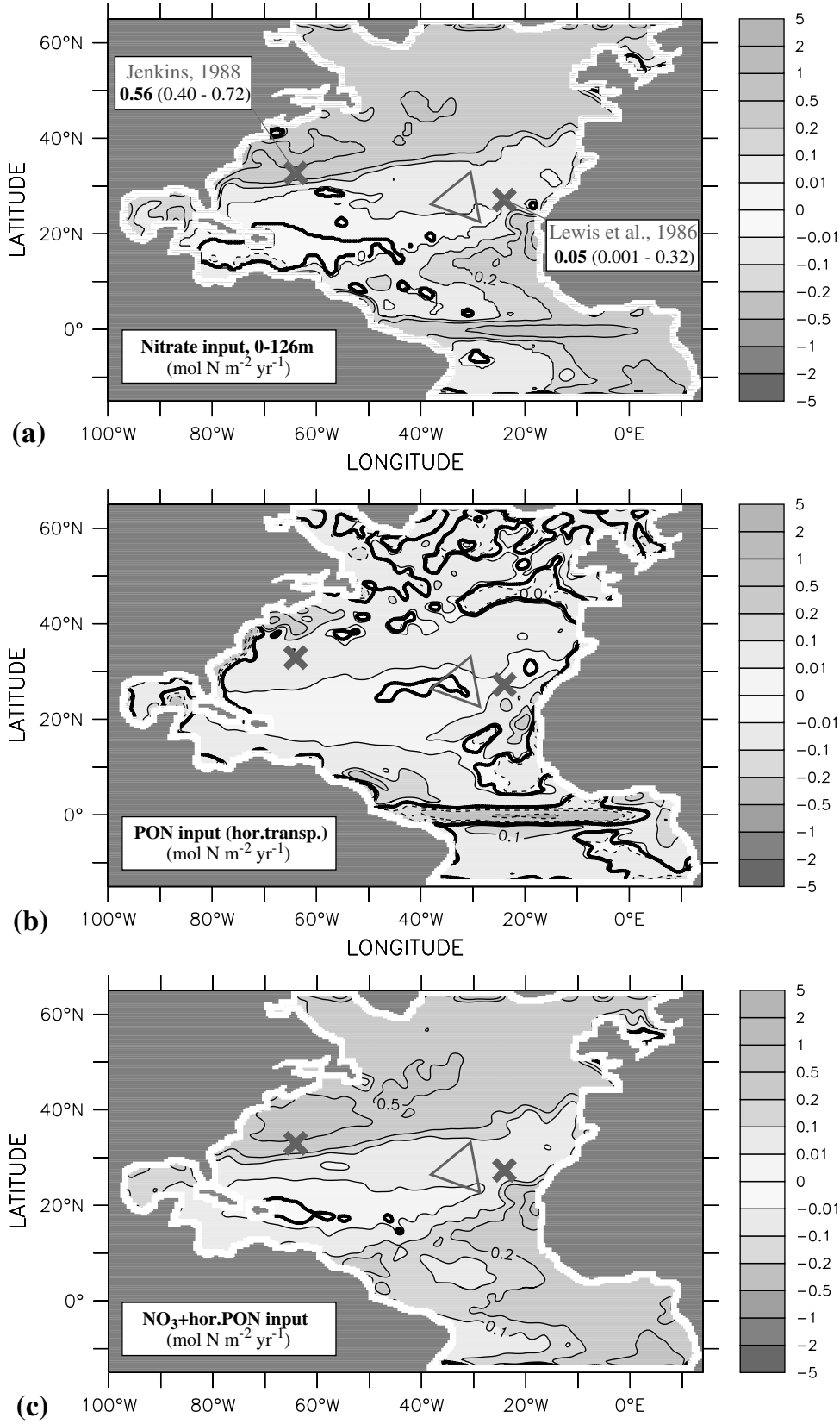

Figure 3. (a) Annual nitrate input into the upper 126 m of the numerical model, averaged over a 5 year integration period. (b) Simulated nitrogen input via horizontal advection of particulate organic nitrogen (PON), i.e., phytoplankton, zooplankton, and detritus. (c) Sum of nitrate input (Figure 3a) and PON input (Figure 3b). Units are mol N m^{-2} yr^{-1}. For reference, observational estimates for nitrate input by *Jenkins* [1988] and *Lewis et al.* [1986] are included as is the position of the Beta Triangle [*Jenkins*, 1982]. See color version of this figure at back of this issue.

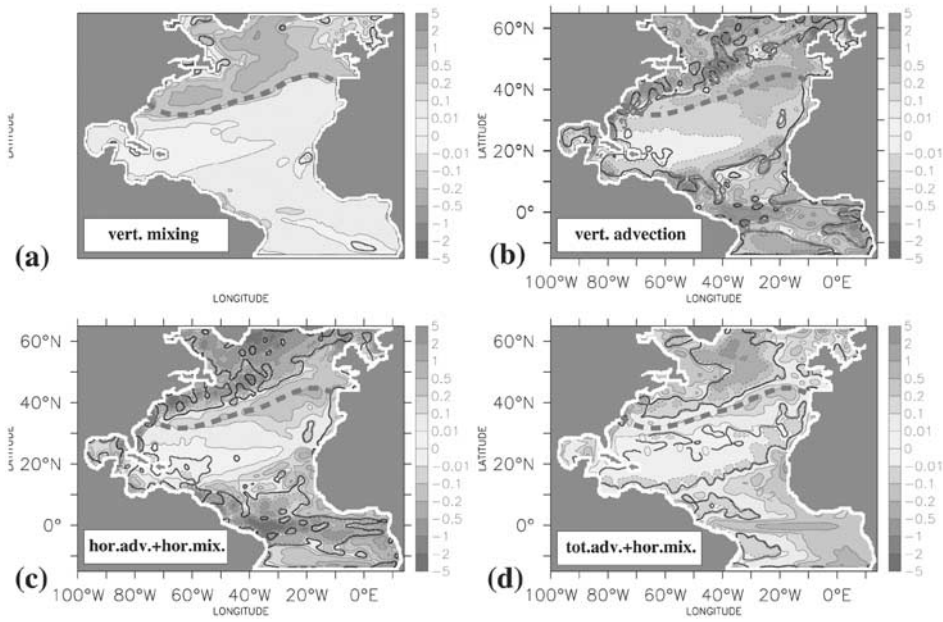

Figure 4. Simulated nitrate supply into the upper 126 m by (a) vertical mixing (including convective mixing), (b) vertical advection, and (c) horizontal advection plus horizontal mixing. (d) The sum of Figures 4a and 4b is displayed. The red dashed line denotes the abrupt step in the winter mixed layer depth shown in Figure 5, the solid red line in Figure 4b is the line of zero mean vertical velocity at z = 126 m of Figure 6. See color version of this figure at back of this issue.

winter mixed layer depths separating regions with deep mixing (>200 m) to the north from the subtropical region where winter mixing does not significantly penetrate the bottom of the euphotic zone (Figure 5). South of this line, nitrate supply by vertical mixing mainly reflects diapycnal mixing in the stratified thermocline. The associated upward nitrate flux is about an order of magnitude smaller than the annual mean nitrate input farther north that is dominated by deep mixing in winter.

[13] The simulated nitrate supply via vertical advection is displayed in Figure 4b. A peculiar feature is that its sign is essentially given by that of the annual mean vertical velocity, which in turn reflects the Ekman downwelling and upwelling induced by the curl of the wind stress (Figure 6). That is, the simulated nitrate input by vertical advection is mainly a result of the large-scale atmospheric wind patterns. In particular, the entire subtropical gyre is a region of Ekman downwelling with an associated export of nitrate out of the euphotic zone. Note that the close relationship between the sign of the annual mean vertical velocity and that of the annual nitrate flux by vertical advection holds despite large temporal variability particularly in the vertical velocity field (Figure 6c). Fluctuations in vertical velocities can arise, for example, from internal waves or mesoscale processes as well as from the seasonally varying Ekman transports. The results shown here indicate that in the context of the present model

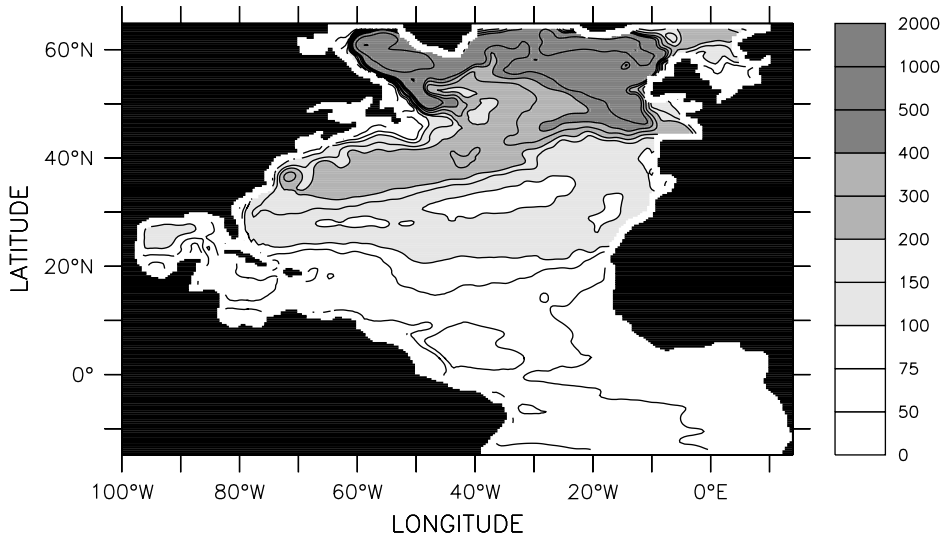

Figure 5. Depth of the winter mixed layer simulated by the model under climatological (1989–1993) forcing. The mixed layer depth is defined by a density criterion ($\Delta\sigma$ = 0.01 kg m^{-3}). Units are meters.

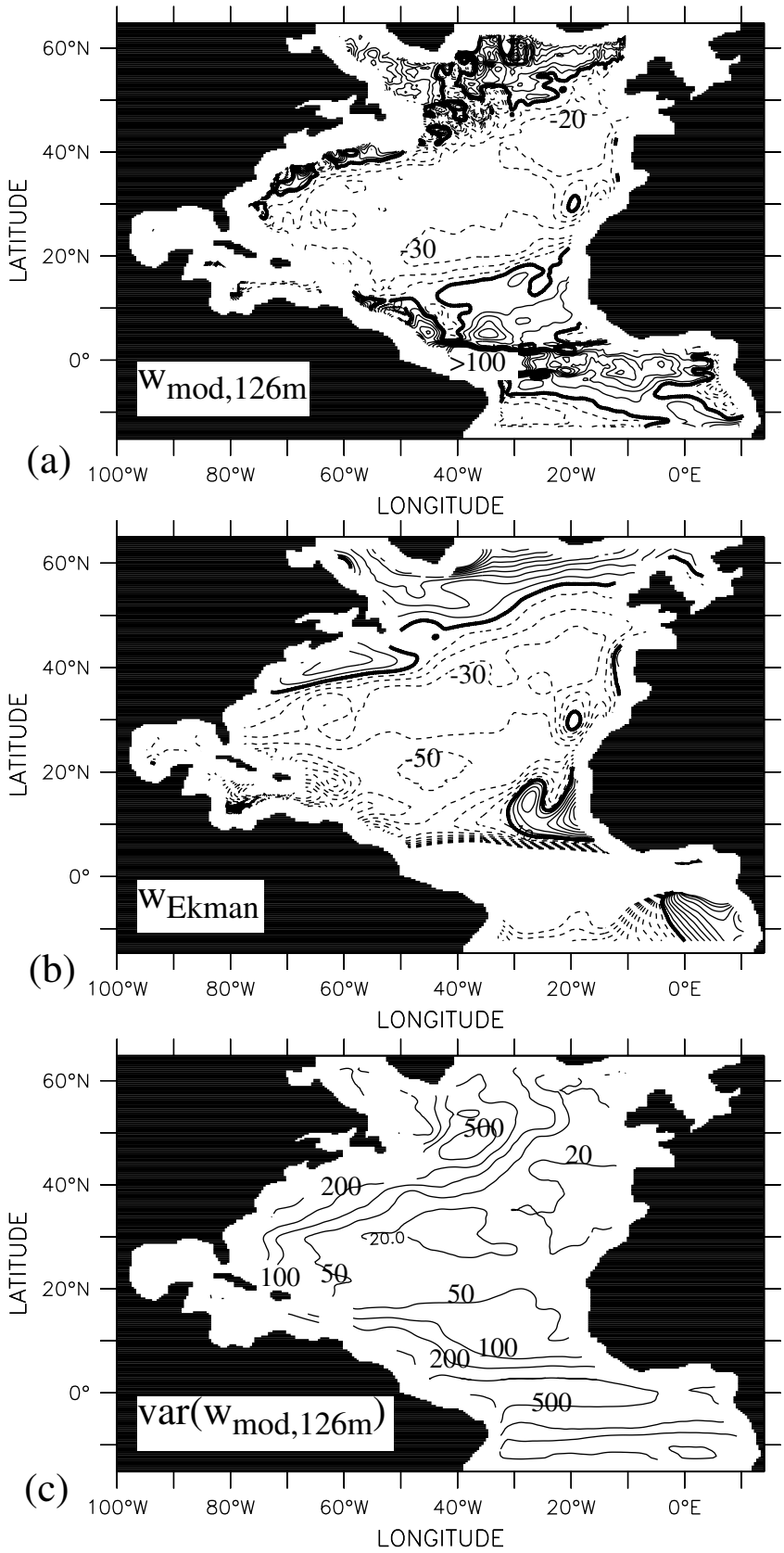
60°N
40°N
20°N
0°
LATITUDE
-20
0
-30
>100
$w_{mod,126m}$
(a)
100°W
80°W
60°W
40°W
20°W
0°E
LONGITUDE
-30
0
-50
w_{Ekman}
(b)
500
20
200
<20.0
100
50
50
100
200
500
$var(w_{mod,126m})$
(c)

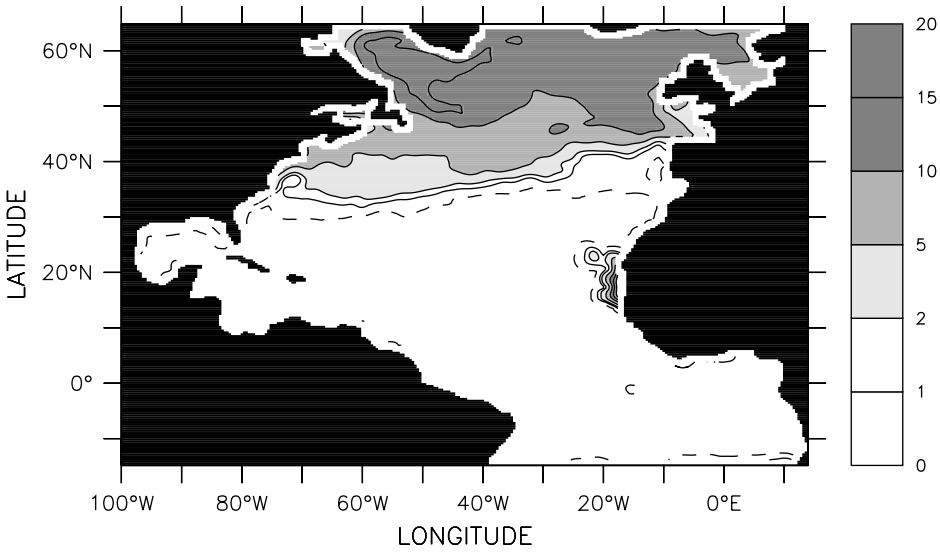

Figure 7. Simulated maximum surface nitrate concentrations in winter. Units are mol m^{-3}. The dashed line refers to the 0.1 mol m^{-3} isoline.

simulation such time-varying processes cannot alter the sign of the large-scale mean vertical nitrate fluxes with respect to those resulting from linear Ekman theory [e.g., *McClain and Firestone*, 1993]. Apart from the sign of the vertical transport, there is, however, little correlation between mean vertical velocities and mean vertical advection of nitrate. For example, nitrate export by vertical advection is lowest in the center of the subtropical gyre where mean vertical velocities (at z = 126 m) are strongest (Figure 6a). While the almost exact coincidence of the lines of zero annual nitrate input by vertical advection and of zero mean vertical velocity suggest that rectifying effects on the simulated nitrate flux are small close to the zero line in Figure 4b, this need not be the case elsewhere.

[14] Nitrate input by vertical advection is largest in the equatorial upwelling region with maximum values of the simulated annual mean nitrate flux across 126 m occuring in the western basin and reaching 2 mol N m^{-2} yr^{-1}. This is even higher than the annual average of nitrate supply by vertical mixing in high latitudes. Coastal upwelling regions off the Iberian peninsula, West Africa, and South America and in the Gulf of Mexico also contribute to the upper ocean's nitrate supply by vertical advection, with annual mean rates generally being less than 1 mol N m^{-2} yr^{-1}.

[15] As a consequence of the continuity equation, nitrate fluxes due to horizontal transport processes are almost everywhere of inverse sign compared to fluxes due to vertical advection (Figure 4c). For example, upwelling regions exhibit a horizontally divergent near-surface flow, ensuring that any upwelled nitrate that escapes immediate biological consumption is exported horizontally. The inverse relation holds for downwelling regions like the subtropical gyre: horizontally convergent near-surface flow transports nutrient-rich water from the outside margins toward the center of the gyre. The near-surface flow comprises the southward Ekman transport induced by generally eastward winds at the northern flank of the subtropical gyre and northward Ekman transport induced by the trade winds at the southern flank [e.g., *Williams and Follows*, 1998]. Note that the analysis of the simulated horizontal nitrate transport does not distinguish between horizontal advection and horizontal diffusion. In a high-resolution model such a distinction would be of little physical relevance because mixing by geostrophic turbulence is assumed to be resolved partially and the amount of mixing required for numerical stability depends primarily on the grid resolution. Hence any lateral nitrate transport that may arise from horizontal mixing by mesoscale eddies is included in this picture.

[16] The sum of simulated nitrate input by vertical advection and that due to horizontal transport processes is shown in Figure 4d. Values are generally positive along the continental margins, at the equator, and south of the band of large input by vertical mixing (Figure 4a) at the northern flank of the subtropical gyre. Near the margins of the subtropical gyre, input by horizontal advection is larger than export by downwelling, in good agreement with the results reported by *Williams and Follows* [1998]. At the northern flank of the subtropical gyre, southward Ekman transport, southward recirculation originating from the Gulf Stream and North Atlantic Current, and also mixing by eddies all act to transfer nutrients into the subtropical gyre. A more detailed inspection of the model results shows that this lateral nutrient flux has a strong seasonal cycle with almost all of the input taking place in winter when the southward Ekman transport is strongest and when mixing is deep and nitrate concentrations are high to the north (Figure 7). Simulated southward fluxes are highest in the eastern basin (>0.2 mol N m^{-2} yr^{-1}) at the northern margin of the subtropical gyre, which is marked by the pronounced step in winter mixed layer depths (Figure 5), but nowhere reach more than a few hundred kilometers into the gyre's interior. At the southeastern flank of the subtropical gyre the model simulates a northward transport of nutrients into the gyre. Compared to the southward transport at the northern flank, this transport reaches an even

Figure 6. (opposite) (a) Five year mean of the vertical velocity simulated by the model at the bottom of the euphotic zone (z = 126 m). (b) Five year mean of the vertical Ekman pumping velocity $w_{\mathrm{Ekman}} = \mathrm{curl}_z(\tau/f)/\rho_w$ computed from the ECMWF wind stress fields for 1989–1993. Since in middle and high latitudes the depth of the Ekman layer is shallower than 50 m, the generally smaller velocities at z = 126 m are consistent with a decrease of mean vertical velocities below the surface Ekman layer. (c) Five year rms variability of simulated vertical velocities at z = 126 m, computed from 15 daily snapshots. Units are m yr^{-1}. The contour interval in Figures 6a and 6b is 10 m yr^{-1}. In Figure 6c, contour lines are at 20, 50, 100, 200, and 500 m yr^{-1}.

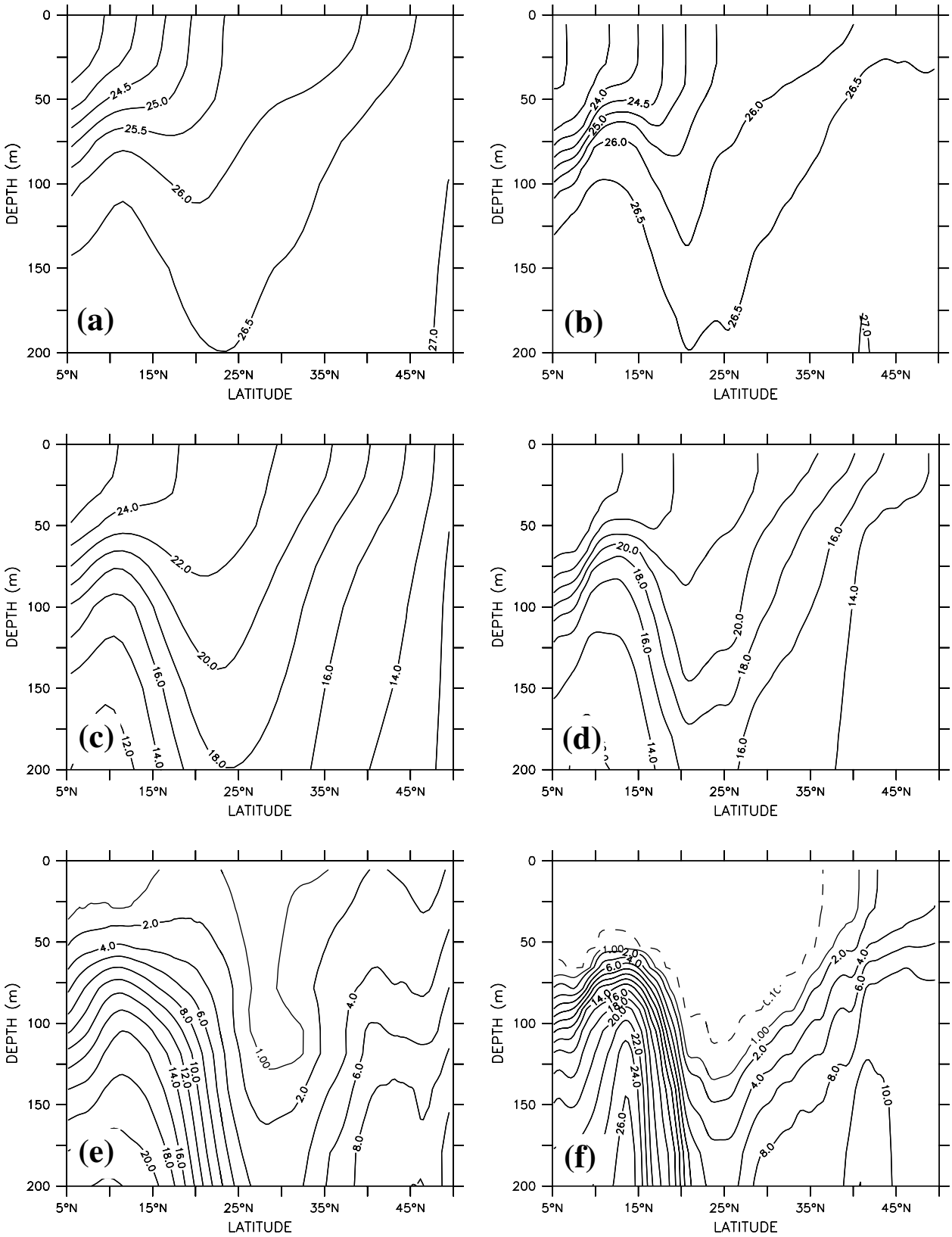

Figure 8. Meridional section along 30°W. All data displayed are zonal averages between 35° and 25°W. (left) Climatological data of (a) potential density and (c) potential temperature taken from the *Levitus and Boyer* [1994] and *Levitus et al.* [1994] atlas and (e) nitrate fields taken from the *Conkright et al.* [1994] atlas. (right) The corresponding 5 year means of (b) potential density, (d) potential temperature, and (f) nitrate as simulated by the model. Units are kg m^{-3} in Figures 8a and 8b, degrees Celsius in Figures 8c and 8d, and mol NO_3 m^{-3} in Figures 8e and 8f. The dashed line in Figure 8f refers to the 0.1 mol NO_3 m^{-3} isocontour (in Figure 8e, concentrations are everywhere above 0.1 mol NO_3 m^{-3}).

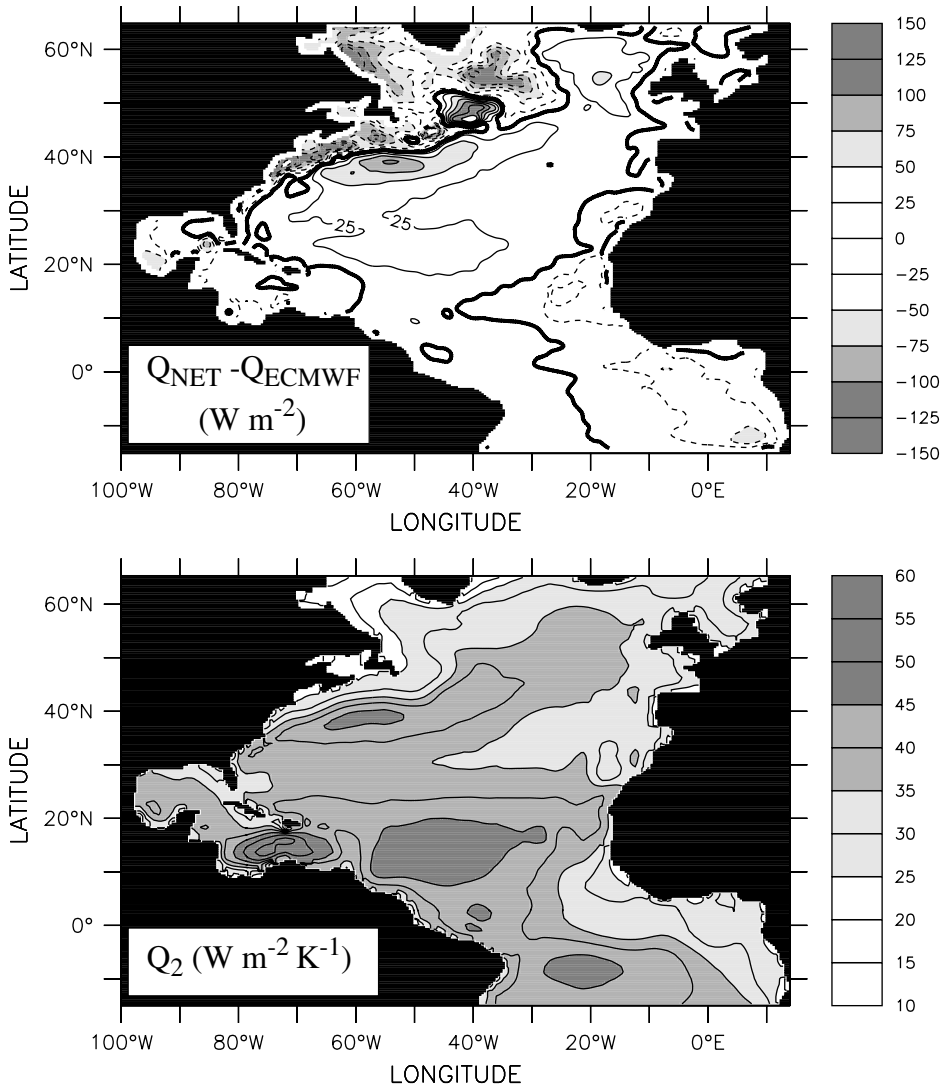

Figure 9. (a) Five year mean of the correction term $Q_2(\mathrm{SST_{obs}} - \mathrm{SST_{mod}})$ for the surface heat flux (equation (1)). (b) Temporally constant flux correction factor Q_2 (described in section 2). Units are W m^{-2} K^{-1}.

shorter distance into the gyre before nutrients are either consumed or subducted.

4. Subtropical Desert Problem

[17] A persistent feature of coupled ecosystem-circulation models of the North Atlantic is that all simulations performed so far, including the coarse-resolution model of *Sarmiento et al.* [1993], the high-resolution experiments reported by OG99, and the altimeter-data assimilation experiment of OG98, have displayed a large region in the subtropical gyre where simulated primary production is less than 1 g C m^{-2} yr^{-1} (Figure 1). This is much lower than is suggested by compilations of in situ measurements that show minimum values of 25 g C m^{-2} yr^{-1} [*Berger*, 1989] or the even higher estimates (>50 g C m^{-2} yr^{-1}) based on satellite ocean color data [e.g., *Behrenfeld and Falkowski*, 1997]. The fact that present biogeochemical models cannot reproduce observed levels of primary production in the oligotrophic subtropical gyre will here be referred to as the subtropical desert problem. An important question to answer is whether the origin of this model deficiency lies in a substantial underestimation of the simulated nutrient supply to the upper ocean or whether errors and oversimplifications in the ecosystem model component are responsible. Errors in the nutrient supply and hence in new production would be of particular concern for a correct assessment of the global nitrogen and carbon cycles, aggravated by the large surface area covered by the subtropical gyre. In the following the modeled nitrate supply will be investigated and compared with observational estimates.

4.1. Indications From the Simulated Heat Balance

[18] A general feature of the subtropical gyre is the bowl-shaped depression of isopycnals toward the gyre's center, shown, for example, for a meridional section along 30°W in Figure 8a. This depression, which is equivalently found for isotherms and isopleths of nitrate concentrations (Figures 8c and 8e), results from Ekman pumping and geostrophically balances the large-scale anticyclonic flow of the gyre. The comparison of the model fields with climatological data shown in Figure 8 reveals that vertical tracer gradients are generally sharper in the model results. This may to some extent be related to the considerable temporal and spatial averaging applied to the climatological data. It might, alternatively, indicate an underestimation of diapycnal mixing by the model. In this case one would expect that simulated surface temperatures in the subtropical gyre, where the net heat flux is positive into the ocean, were too high and that the simulated nitrate input into the euphotic zone was too small. In response to any

deviation of the simulated SST from the "observed" SST [*Reynolds and Smith*, 1994] used to compute the ECMWF reanalysis the chosen formulation of the surface heat flux (1) would counteract by "correcting" the applied ECMWF surface heat flux $Q_{NET}(\mathrm{ECMWF}) = Q_{SOL} + Q_{NSOL}$ by an amount

$$Q_{NET}(\mathrm{model}) - Q_{NET}(\mathrm{ECMWF}) = Q_2(\mathrm{SST_{obs}} - \mathrm{SST_{mod}}) \cdot \quad (2)$$

The 5 year mean of this correction term is displayed in Figure 9. Among other things it shows that over the subtropical gyre the correction term is positive, i.e., the modeled ocean absorbs more heat than is predicted by the ECMWF reanalysis. It further turns out that the large-scale pattern of this flux correction is essentially constant in time. Given the (everywhere positive) values of Q_2 displayed in Figure 9b, this corresponds to an average underestimation of simulated subtropical surface temperatures with respect to observations [*Reynolds and Smith*, 1994] by about half a degree. Note that the correction term (2) combines both model flaws and possible errors in the ECMWF heat fluxes. Although it cannot completely be ruled out that the ECMWF heat fluxes have large-scale errors larger than ±20 W m^{-2}, the sign of the correction term indicates that the model overestimates rather than underestimates the diapycnal transport of heat through the subtropical thermocline. This analysis does not reveal whether the too large diapycnal transport in the model occurs via overestimated vertical mixing, via interactions of mesoscale features like fronts or eddies with the surface mixed layer, or via too large horizontal mixing across sloping isopycnals. Because the transport equations for nutrients and heat are essentially the same (apart from the flux correction applied to biological tracers) and because of the generally close correlation between nitrate and temperature fields in the subtropical gyre, one might expect a similar overestimation of the simulated diapycnal transport of nitrate. It would therefore be difficult to reconcile an underestimation of the simulated input of nitrate to the subtropical gyre with the upper ocean heat budget.

4.2. Comparison With Observational Estimates of the Nitrate Flux

[19] The input of nitrate into the upper 126 m of the model, which here is taken as equivalent of the euphotic zone, is shown in Figure 3a. The locations of two independent observational estimates of vertical nitrate flux are denoted by crosses. In the eastern subtropical Atlantic (28.5°N, 23°W), *Lewis et al.* [1986] used microstructure measurements to deduce vertical diffusivities that were then combined with the observed vertical nitrate gradient. The upward diffusive nitrate flux computed in this way over a 2 week period was consistent with simultaneous ^{15}N uptake measurements of new production in the euphotic zone. Because winter mixing does not penetrate the nutricline in this region, it seems plausible to regard these short-term averages as representative of the annual mean, which then results in a value of 0.05 mol N m^{-2} yr^{-1} with 95% confidence limits 0.001 and 0.32 mol N m^{-2} yr^{-1} for the site of the *Lewis et al.* [1986] measurement. The nitrate flux simulated for the same location by the model amounts to 0.02 mol N m^{-2} yr^{-1}, which is well within the error bars of the observational estimate.

[20] Close to Bermuda (32°N, 64°W), in the northwestern corner of the subtropical gyre, the upward flux of nitrate into the euphotic zone was estimated by *Jenkins* [1988] using tritiugenic helium as a flux gauge. His result (0.56 ± 0.16 mol N m^{-2} yr^{-1}) was an order of magnitude higher than that of *Lewis et al.* [1986], and the two values were not consistent within the error bars. In contrast to the measurements of *Lewis et al.* [1986] that were local in space and in time, geochemical tracer methods like the one applied by *Jenkins* [1988] present an average over large timescales and space scales. This led to the suggestion that mesoscale processes, possibly undersampled in the local measurements while being integrated in the geochemical tracer signal, might explain the discrepancy between the two measurements.

[21] In this respect it is interesting that the 5 year mean nitrate fluxes diagnosed from the high-resolution model at the two measurement sites also differ by more than an order of magnitude (0.02 mol N m^{-2} yr^{-1} at the site of the *Lewis et al.* [1986] estimate and 0.29 mol N m^{-2} yr^{-1} at the site of the *Jenkins* [1988] estimate). While the model result agrees well with the *Lewis et al.* [1986] data, it is below the error bars of the *Jenkins* [1986] estimate near Bermuda. Note that a higher nitrate input of 0.50 mol N m^{-2} yr^{-1}, which is within the observational error bars, was simulated by the control experiment of OG98 with the same model configuration but different atmospheric forcing. This discrepancy may be explained by the different forcing fields representing different phases of the NAO: while the 1989–1993 ECMWF forcing used here corresponds to a phase of a relatively high NAO index, the older climatological data used in the experiments of OG98 (and also the measurements reported by *Jenkins* [1982]) reflect a period during which the NAO index was lower. Near Bermuda a high NAO index is generally associated with shallower winter mixed layers [*Michaels and Knap*, 1996; *Bates*, 2001], and model results suggest a corresponding NAO-related reduction in nitrate supply by some 30% between the 1960s and the 1990s [*Oschlies*, 2001].

[22] An important finding of the above analysis is that the model results obviously can help to reconcile the apparent observational discrepancy between the *Lewis et al.* [1986] and the *Jenkins* [1986] estimates of nitrate input into the euphotic zone of the subtropical gyre. The model-generated basin-wide pattern of nitrate supply to the upper North Atlantic suggests that the seeming inconsistency between the two estimates can be explained by the different locations of the measurements taken. As may be seen in Figure 3a, the two sites are located at different sides of an east-northeastward sloping front that separates the southern part of the subtropical gyre with simulated nitrate input of the order of 0.01 mol N m^{-2} yr^{-1} from the northern part with nitrate fluxes exceeding 0.2 mol N m^{-2} yr^{-1}. As discussed in section 3, this abrupt change in the magnitude of nutrient input is caused by a rapid northward increase in the winter mixed layer depth along the northern margin of the subtropical gyre (Figure 5). Acknowledging some underestimation of the model's eddy activity, that may account for simulated nitrate input being too low by some 30% (OG98), and taking into account possible differences between the atmospheric forcing applied to the model and the atmospheric conditions that affected the observations, the relatively close agreement between simulation and observational estimates at these two locations in the subtropical gyre seems promising. However, there are more data, like those of oxygen consumption described below, that make the picture more complex.

4.3. Comparison With Observational Estimates of Oxygen Consumption

[23] Measurements of apparent oxygen utilization (AOU) in combination with isopycnal gradients of the ^{3}H-^{3}He water mass age have been used to estimate oxygen utilization rates (OURs) in the Beta Triangle [*Jenkins*, 1982, 1987], whose location is indicated in Figure 3. OUR estimates provide a measure of remineralization at depth and hence of export production. For the Beta Triangle, *Jenkins* [1982] obtained a value of 5.7 ± 0.06 mol O_2 m^{-2} yr^{-1}. A more conservative upper limit for the uncertainty in large-scale OUR estimates was given as 20% by *Jenkins and Wallace* [1992]. Assuming an $-O_2$:N ratio of 9.1 ± 0.4 for remineralization [*Minster and Boulahdid*, 1987], this corresponds to a nitrogen remineralization rate of 0.63 ± 0.15 mol N m^{-2} yr^{-1}. This is more than an order of magnitude larger than the mean value of the nearby nitrate supply measurements by *Lewis et al.* [1986] (though their upper 95% confidence limit is 0.32 mol N m^{-2} yr^{-1}). As shown by the compilation of

OUR estimates in the subtropical North Atlantic by *Jenkins and Wallace* [1992], there is little difference in OUR between sites close to Bermuda and the Beta Triangle region. This implies, on the one hand, that there is no apparent discrepancy between oxygen consumption and nitrate supply near Bermuda. On the other hand, this means that despite evidence for considerable regional differences in nitrate supply within the subtropical gyre such differences apparently are not present in the export production. An investigation of sediment trap data by *Lampitt and Antia* [1997] also showed that deep particle export (at 2000 m) in the eastern subtropical North Atlantic was lower by at most a factor 2 compared to that near Bermuda.

[24] A possible explanation to resolve the apparent observational discrepancy between oxygen consumption measurements and the *Lewis et al.* [1986] data may again be different timescales and space scales covered by the different measurement methods. This explanation is, however, not supported by our model results: while the 5 year model average agrees well with the *Lewis et al.* [1986] observations, at the same time the simulated nitrate supply to the euphotic zone in the region of the Beta Triangle (<0.1 mol N m^{-2} yr^{-1}, Figure 3a) is an order of magnitude lower than would be required to balance locally the observed rates of oxygen consumption. An experiment with higher and more realistic levels of eddy activity (OG98) could not significantly alter this picture. Alternative explanations have to be sought to bridge the gap between low nitrate supply and high oxygen consumption rates presumably indicating high export production in the subtropical gyre.

5. Discussion

[25] It has already been suggested that discrepancies between the rate of oxygen consumption at depth and the upward flux of nutrients farther up in the water column may be due to the fact that biogeochemical budgets are inherently three-dimensional rather than one-dimensional: *Rintoul and Wunsch* [1991] computed oxygen and nutrient budgets between zonal sections at 26°N and 34°N in the North Atlantic, from which they inferred that a substantial fraction of oxygen consumption must be a result of remineralization of organic matter fixed outside the area of investigation, presumably north of 34°N, and subsequently advected into the region. In principle, two scenarios of how this can take place are possible. First, there might be an isopycnal transport of organic matter located below the euphotic zone, for example, on the isopycnal surfaces used by *Jenkins* [1982] to compute AOU rates. Presumably, the organic matter associated with such an isopycnal transport would be dissolved organic matter (DOM). Second, there might be a transport of organic matter within the surface layer. Such a transport could be associated with either dissolved or (living) particulate organic matter.

[26] In the following the role of lateral particulate organic nitrogen (PON) transport into the gyre will be investigated within the framework of the numerical model, which at present does not explicitly resolve DOM. Note that in the model formulation, neither phytoplankton nor zooplankton sink. Only the detritus compartment sinks, with a constant velocity of 5 m day^{-1} through the water while being remineralized to nitrate at a constant rate of 0.05 day^{-1} (OG99, Table 2). For this particular model configuration the annual contribution of horizontal PON transport within the upper 126 m is displayed in Figure 3b. Almost everywhere is the simulated near-surface transport of PON in the annual mean dominated by advection of phytoplankton. As discussed by OKG2000, phytoplankton biomass simulated by the model agrees relatively well (within a factor of 2) with observations in different seasons and different biogeochemical provinces. Other components of PON-like bacteria or zooplankton are, however, simulated by the model either not at all or with uncertain accuracy. Quantitative model-derived conclusions about the role of PON advection must therefore be treated cautiously.

[27] The general pattern of the simulated nitrogen input via advection of PON shows positive values in the subtropical gyre, being larger at the margins and becoming smaller toward the interior. This picture is consistent with the horizontally convergent Ekman flow at the surface. In large parts of the subtropical gyre the simulated nitrogen input in the form of PON reaches magnitudes similar to those due to the supply of inorganic nitrate. Nevertheless, the absolute contribution of PON in the model is, for the Beta Triangle region, only of the order 0.01 mol N m^{-2} yr^{-1} and hence does not help explain the observational discrepancy between nitrate input and oxygen consumption rates.

[28] Regions with a larger contribution of the simulated lateral PON transport to the upper ocean nitrogen budget include the equatorial Atlantic, the upwelling region off West Africa, and the Gulf Stream. In the model, PON presents a nitrogen source of about 0.2 mol N m^{-2} yr^{-1} right after the Gulf Stream leaves the American coast. A tongue showing similarly high values originates from the West African upwelling. Along the equator the divergent surface flow fed by the nutrient-rich equatorial upwelling (Figure 4b) exports up to 0.5 mol N m^{-2} yr^{-1} in the form of PON to the north and south of the upwelling region.

[29] Since the present model does not include DOM or atmospheric nitrogen sources, the total rate at which nitrogen is made available for export production is given by the sum of nitrate input and PON transport (Figure 3c). Apart from a small region of slight nitrogen loss (<0.01 mol N m^{-2} yr^{-1}) in the southwestern part of the subtropical gyre, where the model has not fully reached a stable seasonal cycle, the total simulated nitrogen input into the upper 126 m is positive and closely balanced by the export of PON out of the upper 126 m. In contrast, nitrate supply, commonly associated with new production, and export production do not necessarily balance locally. The model results suggest that lateral transport of organic matter within the euphotic zone must be taken into account to close the upper ocean's nitrogen budget, particularly in the equatorial Atlantic, close to the Gulf Stream, near the coastal upwelling off Africa, and at the margins of the subtropical gyre. As a corollary, the total simulated nitrogen supply (Figure 3c) rather than the supply of nitrate (Figure 3a) should be used for comparison with observational estimates of OUR.

6. Conclusions

[30] In this study a numerical model is used to estimate the nitrate supply to the near-surface layer of the North Atlantic Ocean. When setting up the model, particular attention was put on an accurate description of turbulent mixing in the upper ocean, yielding vertical diffusivities in good agreement with recent observations. Horizontal mixing by geostrophic turbulence is to some extent explicitly resolved on the $1/3° \times 2/5°$ model grid, and the effect of the biharmonic subgrid scale mixing parameterization is felt at scales much shorter than in earlier coarse-resolution biogeochemical models. Advection of biological tracers is modeled by a second-order flux-corrected positive scheme with little implicit diffusivity (OG99).

[31] Although the physical model still has some significant deficiencies, for example, the wrong separation of the Gulf Stream, its ability to reproduce closely the surface heat fluxes as taken from the ECMWF reanalysis is promising, especially in the central and eastern North Atlantic (Figure 9). Of particular importance for the model evaluation is the subtropical gyre. Here the coupled model underestimates observed levels of primary production by more than an order of magnitude (OKG2000). A similar error in model-derived estimates of new or export production over the large area covered by the subtropical gyre would have major implications for estimates of global biogeochemical tracer fluxes.

[32] The results presented support the hypothesis that the underestimation of simulated primary production is not caused by an underestimation in the nitrate supply. The model's tendency

to produce slightly too low SSTs over the subtropical gyre indicates an overestimation of diapycnal mixing in this region. Because of the close correspondence of nitracline and thermocline in the subtropics, it seems unlikely that the model should, by whatever possibly unresolved process, underestimate diapycnal mixing of nitrate into the subtropical gyre's euphotic zone. More direct evidence of the model's capability to simulate realistically the nitrate supply to the upper ocean comes from a comparison with direct measurements of nitrate fluxes. Model results agree well with the observations of both *Lewis et al.* [1986] in the eastern part of the gyre and of *Jenkins* [1988] near Bermuda (Figure 3a). This simultaneous agreement helps to reconcile the apparent discrepancy between the two measurements that in different regions of the subtropical gyre produced very different values for the vertical nitrate flux. The model results further suggest that Bermuda is not representative of the oligotrophic regions farther to the south-southeast in the subtropical gyre.

[33] A major observational discrepancy remains, however, between the estimates of oxygen utilization rates in the Beta Triangle region [*Jenkins*, 1982, 1987] and nearby measurements of nitrate supply by *Lewis et al.* [1986]. Although the model results indicate that a local imbalance between new and export production may arise from lateral advection of organic matter into the subtropical gyre, absolute values of the simulated PON input are far too small to explain the imbalance. Other mechanisms must be considered to resolve the seeming discrepancy between high rates of oxygen consumption and low rates of nitrate supply. There is observational support for at least three processes that are not included in the present model configuration and that may help to close the apparent imbalance between new and export production: (1) nitrogen fixation [*Gruber and Sarmiento*, 1997], (2) lateral convergence of dissolved organic nutrients in the surface waters [*Abell et al.*, 2000], and (3) subduction and subsequent oxidation of carbon-rich DOM [*Doval and Hansell*, 2000]. In order to obtain a consistent picture of biogeochemical tracer fields in the subtropical gyre, future work will address the potential contribution of these processes. Results from coupled ecosystem-circulation models like the one presented in this study can, in this evolving process, help to put measurements local in space and in time into a larger coherent picture of how the ocean works.

[34] **Acknowledgments.** I thank Paul Kähler and Wolfgang Koeve for fruitful discussions and Michio Kawamiya, Andrew Dickson, and an anonymous reviewer for comments that helped to improve the manuscript.

References

Abell, J., S. Emerson, and P. Renaud, Distributions of TOP, TON and TOC in the North Pacific subtropical gyre: Implications for nutrient supply in the surface ocean and remineralization in the upper thermocline, *J. Mar. Res.*, *58*, 203–222, 2000.

Barnier, B., L. Siefridt, and P. Marchesiello, Surface thermal boundary condition for a global ocean circulation model from a three-year climatology of ECMWF analyses, *J. Mar. Syst.*, *6*, 363–380, 1995.

Bates, N. R., Interannual variability of oceanic CO_2 and biogeochemical properties in the western North Atlantic subtropical gyre, *Deep Sea Res.*, *Part II*, *48*, 1507–1528, 2001.

Behrenfeld, M. J., and P. G. Falkowski, Photosynthetic rates derived from satellite-based chlorophyll concentration, *Limnol. Oceanogr.*, *42*, 1–20, 1997.

Berger, W. H., Global maps of ocean productivity, in *Productivity of the Ocean: Present and Past*, edited by W. H. Berger, V. S. Smetaceck, and G. Wefer, pp. 429–455, John Wiley, New York, 1989.

Bryan, F. O., and W. R. Holland, A high resolution simulation of the wind- and thermohaline-driven circulation in the North Atlantic Ocean, in *Parameterization of Small-Scale Processes*, edited by P. Müller and D. Henderson, pp. 99–115, Hawaii Inst. of Geophys., Manoa, 1989.

Conkright, M. E., S. Levitus, and T. P. Boyer, *World Ocean Atlas 1994*, vol. 1, *Nutrients, NOAA Atlas NESDIS*, vol. 1, 162 pp., Natl. Oceanic and Atmos. Admin., Silver Spring, Md., 1994.

Dadou, I., V. Garçon, V. Andersen, G. R. Flierl, and C. S. Davis, Impact of the North Equatorial Current meandering on a pelagic ecosystem: A modeling approach, *J. Mar. Res.*, *54*, 311–342, 1996.

Dickson, R. R., J. Lazier, J. Meincke, P. Rhines, and J. Swift, Long-term coordinated changes in the convective activity of the North Atlantic, *Prog. Oceanogr.*, *38*, 241–295, 1996.

Doval, M. D., and D. A. Hansell, Organic carbon and apparent oxygen utilization in the western South Pacific and the central Indian Ocean, *Mar. Chem.*, *68*, 249–264, 2000.

Dugdale, R. C., and J. J. Goering, Uptake of new and regenerated forms of nitrogen in marine production, *Limnol. Oceanogr.*, *12*, 196–206, 1967.

Eppley, R. W., and B. J. Peterson, Particulate organic matter flux and planktonic new production in the deep ocean, *Nature*, *282*, 677–680, 1979.

Falkowski, P. G., D. Ziemann, Z. Kolber, and P. K. Bienfang, Role of eddy pumping in enhancing primary production in the ocean, *Nature*, *352*, 55–58, 1991.

Gaspar, P., Y. Gregoris, and J.-M. Lefevre, A simple eddy kinetic energy model for simulations of the oceanic vertical mixing: Tests at station Papa and Long-Term Upper Ocean Study site, *J. Geophys. Res.*, *95*, 16,179–16,193, 1990.

Gibson, J. K., P. Kallberg, S. Uppala, A. Hernandez, A. Nomura, and E. Serrano, ECMWF Re-Analysis Project report series, 1, ERA description, 72 pp., Eur. Cent. for Medium-Range Weather Forecasting, Reading, U. K., 1997.

Gruber, N., and J. L. Sarmiento, Global patterns of marine nitrogen fixation and denitrification, *Global Biogeochem. Cycles*, *11*, 235–266, 1997.

Haney, R. L., Surface thermal boundary condition for ocean circulation models, *J. Phys. Oceanogr.*, *1*, 241–248, 1971.

Hurrell, J. W., Decadal trends in the North Atlantic Oscillation: Regional temperatures and precipitation, *Science*, *269*, 676–679, 1995.

Jenkins, W. J., Oxygen utilization rates in North Atlantic subtropical gyre and primary production in oligotrophic systems, *Nature*, *300*, 246–248, 1982.

Jenkins, W. J., ^{3}H and ^{3}He in the Beta Triangle: Observations of gyre ventilation and oxygen utilization rates, *J. Phys. Oceanogr.*, *17*, 763–783, 1987.

Jenkins, W. J., Nitrate flux into the euphotic zone near Bermuda, *Nature*, *331*, 521–523, 1988.

Jenkins, W. J., and D. W. R. Wallace, Tracer based inferences of new production in the sea, in *Primary Productivity and Biogeochemical Cycles in the Sea*, edited by P. G. Falkowski and A. D. Woodhead, pp. 299–318, Plenum, New York, 1992.

Lampitt, R. S., and A. N. Antia, Particle flux in deep seas: Regional characteristics and temporal variability, *Deep Sea Res., Part I*, *44*, 1377–1403, 1997.

Ledwell, J. R., A. J. Watson, and C. S. Law, Evidence for slow mixing across the pycnocline from an open-ocean tracer-release experiment, *Nature*, *364*, 701–703, 1993.

Ledwell, J. R., A. J. Watson, and C. S. Law, Mixing of a tracer in the pycnocline, *J. Geophys. Res.*, *103*, 21,499–21,529, 1998.

Levitus, S., and T. Boyer, *World Ocean Atlas 1994*, vol. 4, *Temperature, NOAA Atlas NESDIS*, vol. 4, 129 pp., Natl. Oceanic and Atmos. Admin., Silver Spring, Md., 1994.

Levitus, S., R. Burgett, and T. Boyer, *World Ocean Atlas 1994*, vol. 3, *Salinity, NOAA Atlas NESDIS*, vol. 3, 111 pp., Natl. Oceanic and Atmos. Admin., Silver Spring, Md., 1994.

Lewis, M. R., W. G. Harrison, N. S. Oakey, D. Herbert, and T. Platt, Vertical nitrate fluxes in the oligotrophic ocean, *Science*, *234*, 870–873, 1986.

McClain, C. R., and J. Firestone, An investigation of Ekman upwelling in the North Atlantic, *J. Geophys. Res.*, *98*, 12,327–12,339, 1993.

McGillicuddy, D. J., Jr., and A. R. Robinson, Eddy-induced nutrient supply and new production in the Sargasso Sea, *Deep Sea Res., Part I*, *44*, 1427–1450, 1997.

McGillicuddy, D. J., Jr., A. R. Robinson, D. A. Siegel, H. W. Jannasch, R. Johnson, T. D. Dickey, J. McNeil, A. F. Michaels, and A. H. Knap, Influence of mesoscale eddies on new production in the Sargasso Sea, *Nature*, *394*, 263–266, 1998.

Michaels, A. F., and A. H. Knap, Overview of the U.S. JGOFS Bermuda Atlantic Time-series Study and the Hydrostation S program, *Deep Sea Res., Part II*, *43*, 157–198, 1996.

Minster, J. F., and M. Boulahdid, Redfield ratios along isopycnal surfaces—A complementary study, *Deep Sea Res.*, *Part A*, *34*, 1981–2003, 1987.

Oschlies, A., NAO-induced long-term changes in nutrient supply to the surface waters of the North Atlantic, *Geophys. Res. Lett.*, *28*, 1751–1754, 2001.

Oschlies, A., and V. Garçon, Eddy induced enhancement of primary production in a model of the North Atlantic Ocean, *Nature*, *394*, 266–269, 1998.

Oschlies, A., and V. Garçon, An eddy-permitting coupled physical-biological model of the North Atlantic, 1, Sensitivity to advection numerics and mixed layer physics, *Global Biogeochem. Cycles*, *13*, 135–160, 1999.

Oschlies, A., W. Koeve, and V. Garçon, An eddy-permitting coupled physical-biological model of the North Atlantic, part II, Ecosystem dynamics and comparison with satellite and JGOFS local studies data, *Global Biogeochem. Cycles*, *14*, 499–523, 2000.

Pacanowski, R., K. Dixon, and A. Rosati, The G. F. D. L. Modular Ocean Model users guide version 1, *Tech. Rep. 2*, GFDL Ocean Group, Geophys. Fluid Dyn. Lab., Princeton, N. J., 1991.

Polzin, K. L., J. M. Toole, and R. W. Schmitt, Finescale parameterizations of turbulent dissipation, *J. Phys. Oceanogr.*, *25*, 306–328, 1995.

Reynolds, R. W., and T. M. Smith, Improved global sea surface temperature analysis using optimum interpolation, *J. Clim.*, *7*, 929–948, 1994.

Rintoul, S. R., and C. Wunsch, Mass, heat, oxygen and nutrient fluxes and budgets in the North Atlantic Ocean, *Deep Sea Res.*, *Part A*, *38,* suppl., 355–377, 1991.

Sarmiento, J. L., G. Thiele, R. M. Key, and W. S. Moore, Oxygen and nitrate new production and remineralization in the North Atlantic, *J. Geophys. Res.*, *95*, 18,303–18,315, 1990.

Sarmiento, J. L., R. D. Slater, M. J. R. Fasham, H. W. Ducklow, J. R. Toggweiler, and G. T. Evans, A seasonal three-dimensional ecosystem model of nitrogen cycling in the North Atlantic euphotic zone, *Global Biogeochem. Cycles*, *7*, 417–450, 1993.

Williams, R. G., and M. J. Follows, The Ekman transfer of nutrients and maintenance of new production over the North Atlantic, *Deep Sea Res., Part I*, *45*, 461–489, 1998.

A. Oschlies, Institut für Meereskunde an der Universität Kiel, Düsternbrooker Weg 20, 24105 Kiel, Germany.

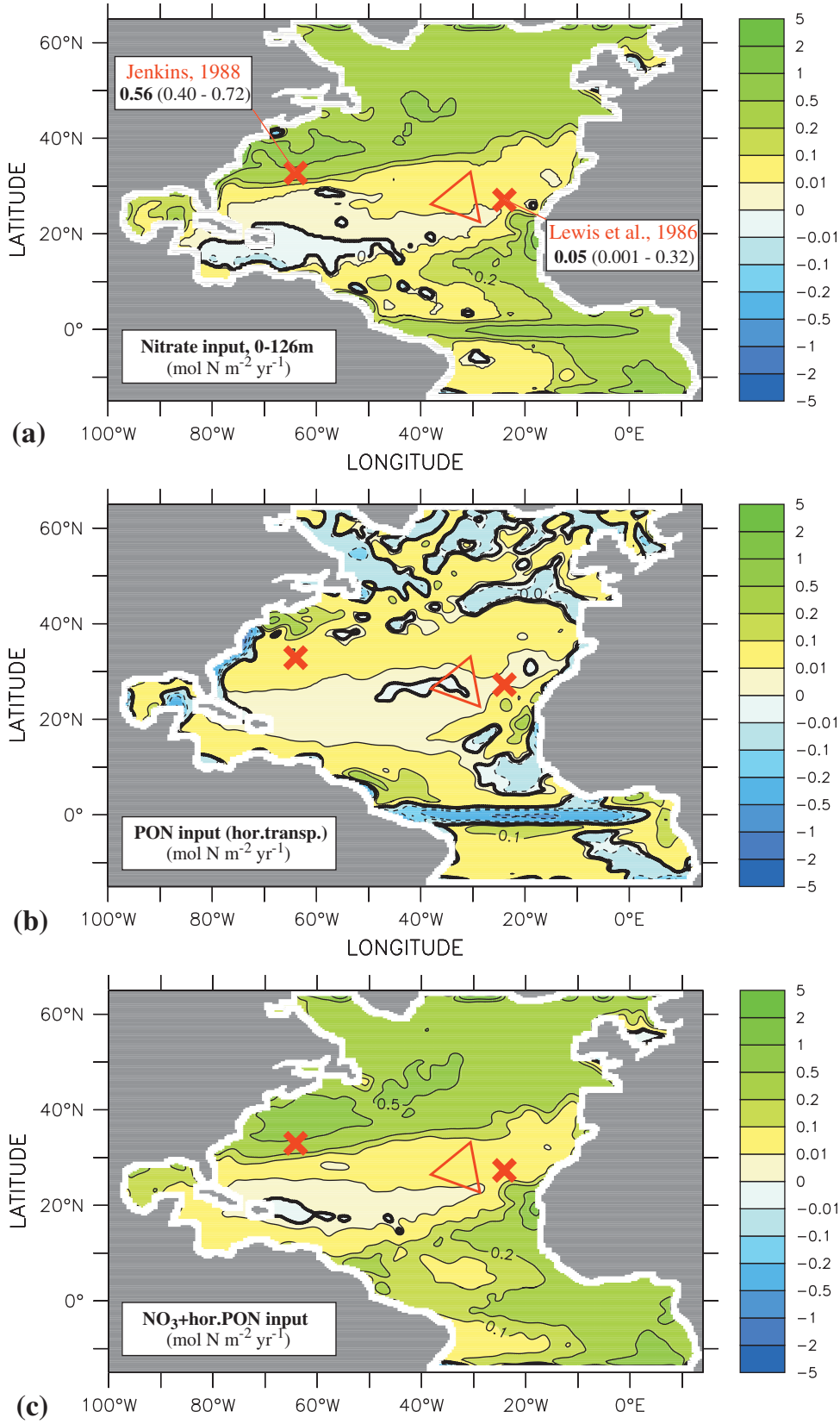

Figure 3. (a) Annual nitrate input into the upper 126 m of the numerical model, averaged over a 5 year integration period. (b) Simulated nitrogen input via horizontal advection of particulate organic nitrogen (PON), i.e., phytoplankton, zooplankton, and detritus. (c) Sum of nitrate input (Figure 3a) and PON input (Figure 3b). Units are mol N m^{-2} yr^{-1}. For reference, observational estimates for nitrate input by *Jenkins* [1988] and *Lewis et al.* [1986] are included as is the position of the Beta Triangle [*Jenkins*, 1982].

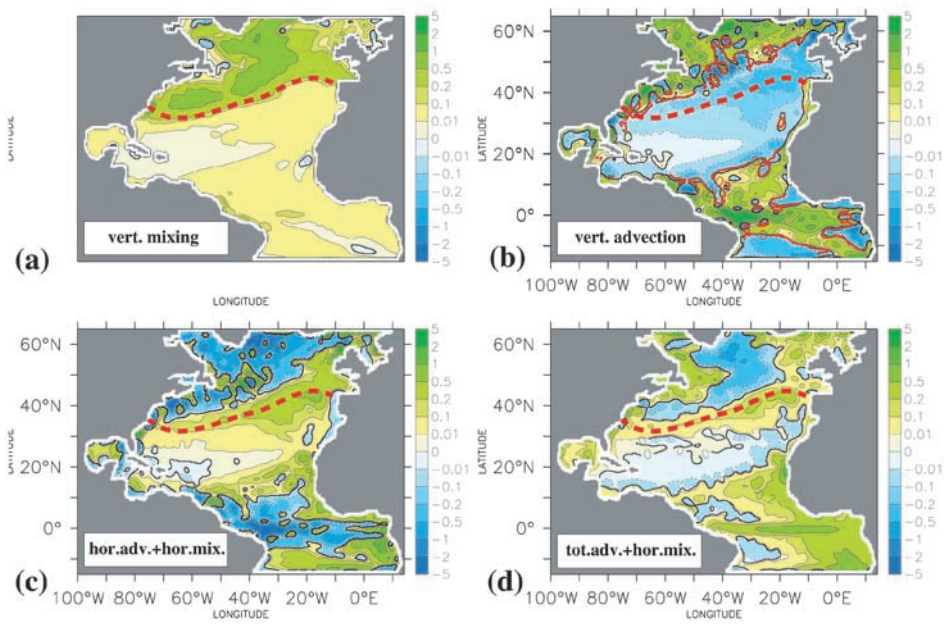

Figure 4. Simulated nitrate supply into the upper 126 m by (a) vertical mixing (including convective mixing), (b) vertical advection, and (c) horizontal advection plus horizontal mixing. (d) The sum of Figures 4a and 4b is displayed. The red dashed line denotes the abrupt step in the winter mixed layer depth shown in Figure 5, the solid red line in Figure 4b is the line of zero mean vertical velocity at z = 126 m of Figure 6.